

University of Groningen

Adhesion of polymer coatings studied by laser-induced delamination

Fedorov, A.; De Hosson, J. Th. M.

Published in:
Journal of Applied Physics

DOI:
[10.1063/1.1929858](https://doi.org/10.1063/1.1929858)

IMPORTANT NOTE: You are advised to consult the publisher's version (publisher's PDF) if you wish to cite from it. Please check the document version below.

Document Version
Publisher's PDF, also known as Version of record

Publication date:
2005

[Link to publication in University of Groningen/UMCG research database](#)

Citation for published version (APA):

Fedorov, A., & De Hosson, J. T. M. (2005). Adhesion of polymer coatings studied by laser-induced delamination. *Journal of Applied Physics*, 97(12), 123510-1 - 123510-7. [123510].
<https://doi.org/10.1063/1.1929858>

Copyright

Other than for strictly personal use, it is not permitted to download or to forward/distribute the text or part of it without the consent of the author(s) and/or copyright holder(s), unless the work is under an open content license (like Creative Commons).

The publication may also be distributed here under the terms of Article 25fa of the Dutch Copyright Act, indicated by the "Taverne" license. More information can be found on the University of Groningen website: <https://www.rug.nl/library/open-access/self-archiving-pure/taverne-amendment>.

Take-down policy

If you believe that this document breaches copyright please contact us providing details, and we will remove access to the work immediately and investigate your claim.

Downloaded from the University of Groningen/UMCG research database (Pure): <http://www.rug.nl/research/portal>. For technical reasons the number of authors shown on this cover page is limited to 10 maximum.

Adhesion of polymer coatings studied by laser-induced delamination

A. Fedorov and J. Th. M. De Hosson^{a)}

Department of Applied Physics, Materials Science Centre, and the Netherlands Institute for Metals Research, University of Groningen, Nijenborgh 4, 9747 AG Groningen, The Netherlands

(Received 28 July 2004; accepted 21 April 2005; published online 20 June 2005)

This paper concentrates on the laser-induced delamination technique, aimed at measuring the practical work of adhesion of thin polymer coatings on metal substrates. In this technique an infrared laser-pulsed beam is used to create an initial blister. Upon increasing the pulse intensity, the size of the blister grows, resulting in partial delamination of the film. In this work the blister profiles and the blister pressure were obtained from independent measurements. Alongside experiments, a simple model is developed to provide the equations necessary for calculating the blister strain energy, height, and the gas pressure inside the blister. The model is essentially based on an elastic behavior of the polymer film. The blister height and the blister pressure predicted by the model were confronted with the experimental observations and a fair agreement was found. The adhesion properties of the polyethylene terephthalate films on a steel substrate were characterized in terms of the maximum stress required for delamination and the practical work of adhesion. The relation between the two are discussed. Because the blister formation and subsequent delamination take place on a time scale of microseconds, it is argued that the viscous properties of the film do not manifest on this time scale and the contribution of plastic deformation of the film is rather small.
© 2005 American Institute of Physics. [DOI: 10.1063/1.1929858]

I. INTRODUCTION

Characterization of adhesion of polymer coatings to metal substrates is of great importance in many modern industrial applications. Often, already laminated metal sheets at different steps of processing are subjected to mechanical, thermal, and chemical treatments. Each of these treatments can alter the adhesion of the coating. Various experimental techniques aimed at characterizing the adhesion properties of polymer coatings have been developed. Among those the blister test has become a well-established and widely used technique.^{1–5} In the conventional blister test, injection of gas or liquid into the space between the film and the substrate results into the formation of a blister. The drawback of this method is that the substrate has to be prepared prior to the lamination process, e.g., a hole has to be drilled in the substrate to allow the gas flow. Thus already coated samples, As received cannot be examined.

In the proposed laser-induced delamination technique, the blisters are formed with the help of an infrared (IR) pulsed laser and no special preparation of the samples is required. By increasing stepwise the power of the laser pulse, high pressure of gas inside the blister can be achieved, sufficient to result in further delamination of the coating. The technique was proposed by Meth *et al.*,⁶ where the adhesion properties of sandwichlike films, consisting of a top IR transparent and a bottom opaque layer, were studied. In these experiments the bottom opaque layer evaporated creating a blister. Later similar experiments were performed on purely IR transparent polyethylene terephthalate (PET) coatings.⁷ The energy absorbed by the steel substrate was enough to form the blisters. The experimental technique presented in

this work has substantial advantages. First, the shape of the blisters has a cylindrical symmetry. That facilitates the measuring procedure of the blister profile and enables the use of a simple two-dimensional (2D) elastic model to analyze the results. Second, by using a mask an unirradiated strip in the middle part of the blister is formed. The strip is not exposed to the laser irradiation and is delaminated purely under the stresses created in the caps of the adjacent blisters.

In the presented work the blister profile and the blister pressure were independently measured. The typical height of a blister, which is about 20–30 μm , was measured with high accuracy, i.e., less than 0.1 μm , with a standard stylus profiler. The measurements of the pressure inside the blister are less straightforward and also less accurate. The blister pressure has also been obtained from the blister profile measurements by applying a model based on linear elasticity.

Usually the work applied to produce delamination is split in two contributions,

$$G = W_a + \psi. \quad (1)$$

The first term at the right-hand side is associated with the minimum work required to separate the coating from the substrate. The second term ψ comprises all extra work produced during the delamination. There is less agreement about the terminology of G . Different wording can be found in the literature, e.g., total work of fracture,⁸ practical work of adhesion or fracture energy,⁹ macroscopic work of fracture,¹⁰ total-energy input,¹¹ crack extension force,² and interfacial toughness.¹² In this paper G is called the practical work of adhesion. W_a is usually called the work of adhesion or true (thermodynamic) adhesive energy,^{8,9,12,13} as it is defined by the Young–Dupré expression for the contact angle in classical thermodynamics.¹³ This definition implies that the system stays in thermodynamic equilibrium during delamination. In

^{a)}Electronic mail: j.t.m.de.hosson@rug.nl

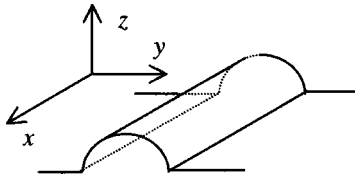


FIG. 1. Cylindrical geometry of a blister. The advantage of the cylindrical geometry is that the results of the profile measurements (taken parallel to the y axis) are not sensitive to the x location of the point, from where the profile is taken.

delamination experiments, however, the detachment of the coating is accomplished via the process of crack propagation along the interface and this process can be considered being neither equilibrium nor reversible. Therefore, the first term on the right-hand side of Eq. (1) is also called the true adhesive fracture energy,¹¹ emphasizing that delamination is essentially a fracture process. This definition allows some dissipation of energy due to plastic deformation around the crack tip, crazing or other processes, localized at the interface and accompanying the propagation of the crack. This value also depends on the mode mixity of the crack opening.¹² Other possibilities of energy dissipation, not localized at the interface and not related to the propagation of the crack, are accounted for in ψ . A typical example of such energy dissipation is the plastic deformation of a film during a peel test, as extensively discussed elsewhere.^{10,11}

In the proposed method the contribution of the plastic deformations denoted by ψ is expected to be rather limited for the following reasons. First, the stress components in the bulk of the polymer are below the yield stress of the polymer under study. Second, the formation of the blisters and subsequent delamination take place on a time scale of microseconds, which is much shorter than the typical relaxation times of polymers at room temperature. As a consequence the viscous properties of the polymer do not have enough time to manifest. Plastic deformation of the blister cap has been observed but this process takes place over a time scale of days. Provided the profilometry measurements are performed within a couple of hours after the blisters are created, the effect of shrinkage of the blister cap can be ignored.

II. THIN PLATE MODEL

A cylindrical blister aligned with the x axis can be described as a thin plate clamped along the boundaries parallel to the x axis (see Fig. 1). Within the Kirchhoff assumptions¹⁴ the governing equation for deflection w of a thin plate under normal uniform pressure p' in 2D is written as

$$\frac{d^4 w}{dy^4} = \frac{p'}{D}, \quad (2)$$

where $D = Et^3/12(1-\nu^2)$ is the flexural rigidity, E is the modulus of elasticity, ν is Poisson's ratio, and t is the film thickness. Naturally the blisters are overpressurized and the pressure excess over the atmospheric pressure is denoted by p' . Then the absolute pressure inside the blister is $p = p' + p_{\text{atm}}$.

The corresponding boundary conditions are as follows:

$$w = 0, \quad \frac{dw}{dy} = 0, \quad \text{at } y = -\frac{b}{2} \quad (3)$$

and

$$y = \frac{b}{2},$$

where b is the dimension of the blister along the y axis. The solution for this boundary problem is

$$w(y) = \frac{p'b^4}{24D} \left[\left(\frac{y}{b} \right)^2 - \frac{1}{4} \right]^2. \quad (4)$$

The maximum height of the blister is

$$H = w \Big|_{y=0} = \frac{p'b^4}{24D} \frac{1}{16}. \quad (5)$$

This expression will be used to evaluate the blister pressure from the measurements of the blister profile,

$$p = p_{\text{atm}} + \frac{24D \cdot 16H}{b^4}. \quad (6)$$

The blister shape can also be expressed in terms of the height,

$$w(y) = 16H \left[\left(\frac{y}{b} \right)^2 - \frac{1}{4} \right]^2. \quad (7)$$

The stresses σ_x and τ_{xy} are equal to zero because of the symmetry. The only nonzero stress obtained from Hooke's law is σ_y ,

$$\sigma_y = -\frac{Ez}{1-\nu^2} \frac{p'b^2}{6D} \left[3 \left(\frac{y}{b} \right)^2 - \frac{1}{4} \right]. \quad (8)$$

The stresses σ_z , τ_{xz} , and τ_{yz} are considered to be negligibly small and are not related to the corresponding strains by Hooke's law (since the latter are zero in the Kirchhoff approach). However, these stresses can still be found by integrating the equations of equilibrium,

$$\tau_{xz} = 0, \quad (9)$$

$$\tau_{yz} = \frac{E}{2(1-\nu^2)} \left(z^2 - \frac{t^2}{4} \right) \frac{p'y}{D},$$

$$\sigma_z = -\frac{E}{2(1-\nu^2)} \left(\frac{z^3}{3} - \frac{t^2}{4}z - \frac{t^3}{12} \right) \frac{p'}{D} - p'. \quad (10)$$

It is easy to check that at the internal surface of the blister $\sigma_z = -p$. The component σ_y provides the biggest contribution to the strain energy of the film. At the bottom surface of the film ($z = -t/2$), the stress is compressive at the center of the blister, and tensile at the clamped boundaries. The stress on the top surface of the film ($z = t/2$) has the same absolute value but the opposite sign. In the middle plane, as it is assumed in the stiff plate theory, the stresses are zero. The maximum stress in the film is achieved for the σ_y component at the clamped boundaries ($y = -b/2$ and $y = b/2$), at the interface with the substrate ($z = -t/2$);

$$\sigma_y^{\max} = \frac{Et}{(1-\nu^2)24D} p'b^2 \quad (11)$$

More detailed analysis of the stresses at the blister boundaries can be performed with a finite element model. This work is in progress and will be published elsewhere.

Because in practice the blisters have a finite length, it is convenient to introduce the blister length a , measured in the x direction. The elastic strain energy in this case is

$$U_y = \frac{(p')^2 ab^5}{20 \cdot 24D} \quad (12)$$

The volume of the blister has the following expression:

$$V = \frac{ap'b^5}{30 \cdot 24D} \quad (13)$$

Note that in reality the blister is also clamped at the boundaries $x=0$ and $x=a$. However, if $a \gg b$ the introduced error is limited.

Upon increasing the blister pressure, the blister can grow through further delamination of the film. The work produced by the gas at constant temperature is given by the change in the Helmholtz free energy $dF = -pdV$. Delamination also causes relaxation of the strain energy of the blister cap U . Thus the condition for delamination is as follows:

$$-(dF + dU) = pdV - dU \geq GdS, \quad (14)$$

where G is the practical work of adhesion or the fracture energy. The elementary change of the blister area is $dS = a \cdot db$. The other differentials involved are derived below.

Assume that during delamination the blister width changes from b_0 to b . From the condition $pV = \text{const}$ the behavior of the overpressure p' inside the blister as a function of the blister width is obtained,

$$p'(b) = -\frac{p_{\text{atm}}}{2} + \sqrt{\left(\frac{p_{\text{atm}}}{2}\right)^2 + (p_{\text{atm}} + p'_0)p'_0 \left(\frac{b_0}{b}\right)^5}, \quad (15)$$

where p'_0 is the initial overpressure in the blister. The elementary change in the strain energy dU according to Eq. (12) has two contributions,

$$dU = \left(\frac{\partial U}{\partial b}\right)db + \left(\frac{\partial U}{\partial p'}\right)\left(\frac{\partial p'}{\partial b}\right)db. \quad (16)$$

The first term is positive while the second term is negative because of $(\partial p'/\partial b) < 0$. The second term dominates and ensures that the $(dU/db) < 0$; the blister cap relaxes during the delamination. By taking all required derivatives at $b=b_0$, the expression for dU normalized by dS can be obtained,

$$\frac{dU}{dS} \Big|_{b=b_0} = -\frac{(p'_0)^2 b_0^4}{4 \cdot 24D} \left(\frac{p_{\text{atm}}}{p_{\text{atm}} + 2p'_0}\right). \quad (17)$$

Here the following transformation is used to simplify the result:

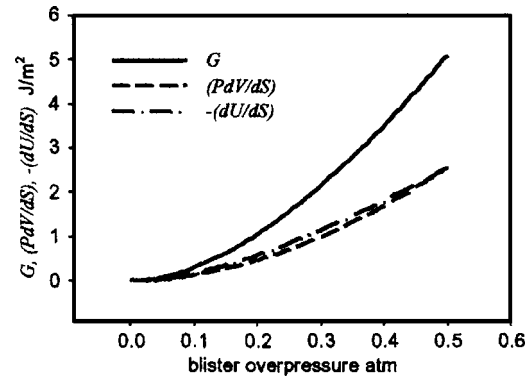


FIG. 2. Practical work of adhesion is shown as a function of the blister pressure. Both contributions in the practical work of adhesion: work of the gas inside the blister and the relaxation of the blister cap are shown separately.

$$\begin{aligned} \frac{\partial p'}{\partial b} \Big|_{b=b_0} &= -\frac{5(p_{\text{atm}} + p'_0)p'_0 \left(\frac{1}{b_0}\right)}{\sqrt{p_{\text{atm}}^2 + 4(p_{\text{atm}} + p'_0)p'_0}} \\ &= \frac{5(p_{\text{atm}} + p'_0)p'_0 \left(\frac{1}{b_0}\right)}{p_{\text{atm}} + 2p'_0}. \end{aligned} \quad (18)$$

By using the expression for the blister volume, Eq. (13), in the similar way the expression for the elementary work produced by the gas inside the blister is calculated,

$$\frac{dF}{dS} \Big|_{b=b_0} = -\frac{b_0^4 (p'_0)^2 p_{\text{atm}} + p'_0}{6 \cdot 24D p_{\text{atm}} + 2p'_0}. \quad (19)$$

Consequently, the practical work of adhesion is the sum of those two contributions,

$$G = \frac{b_0^4 (p'_0)^2 (5p_{\text{atm}} + 2p'_0)}{288D p_{\text{atm}} + 2p'_0}. \quad (20)$$

The practical work of adhesion is plotted in Fig. 2 as a function of the blister pressure. The initial blister width is taken as $b_0 = 1$ mm, a typical value used in the experiments. Both contributions, coming from the changes in the Helmholtz free energy of the gas and the strain energy of the blister cap, are also shown separately.

As it was already mentioned, delamination, which takes place in the laser-induced blister tests, is essentially a crack propagation process, which is not reversible and is unlikely to go through equilibrium states. Therefore, the thermodynamic description presented above has to be taken with caution. The aim of this section is to relate the maximum stresses at the blister boundary required for delamination, which can be derived from the test, to the practical work of adhesion, usually cited in the literature. In Fig. 3 both values are plotted against each other.

III. EXPERIMENTAL PROCEDURE

The method of the laser-induced delamination is schematically illustrated in Fig. 4. A sample with an IR transparent polymer film on a steel substrate is subjected to a series

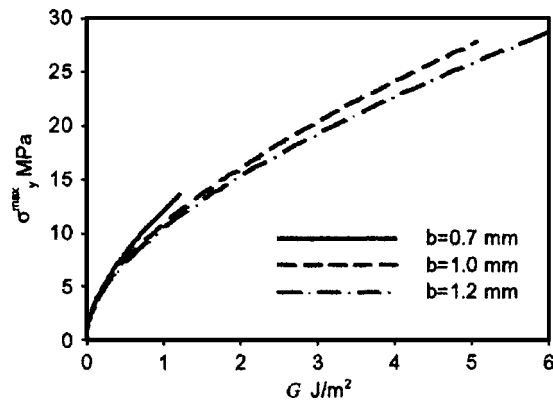


FIG. 3. Relation between the practical work of adhesion and the tensile stress required for delamination is presented. The calculations are carried out for three cases of three different blister size: $b=0.7$, 1.0, and 1.2 mm.

of IR laser pulses. Every shot is performed on a newly unirradiated area. The shots are performed through the mask. The essential feature of the mask is to create a shadowed region in the middle of the irradiated area. The intensity of the first laser pulse in the series is chosen in a way that only at the areas exposed to the laser radiation the blisters are formed. The shadowed region remains attached to the substrate (shot 1). With every next shot in the series the intensity of the laser pulse increases, until the delamination of the shadowed region takes place (shot 3). The corresponding blister pressure p and the blister height H are used to calculate the work of adhesion.

A Surelite neodymium: yttrium aluminum garnet (Nd:YAG) IR laser from Continuum was used to produce the IR pulses. The maximum energy of the pulse is 0.5 J, the pulse duration is 5 ns, and the wavelength is $1.064 \mu\text{m}$. The original beam of 6 mm in diameter was expanded three times. After the expander the high-power attenuator from Del Mar Ventures was used to vary the intensity of the beam. The attenuator comprised the UV grade fused silica wheel with the diffraction gratings. Further the lens was used to focus the beam on the sample. Usually the sample was placed in out-of-focus position, thus the intensity of the beam at the sample could be varied both by the attenuator and the position of the sample with respect to the focus point. From the

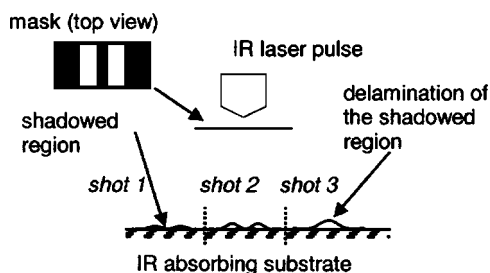


FIG. 4. Schematic presentation of the laser induced (assisted) delamination technique. A series of subsequent laser shots are performed through the mask shown at the left top. The laser-pulse intensity gradually increases with each shot. Shots 1 and 2 correspond to the laser-pulse intensity before the shadowed region is delaminated from the substrate. Shot 3 corresponds to the intensity when the area not exposed to the laser irradiation is delaminated and both blisters merge in one.

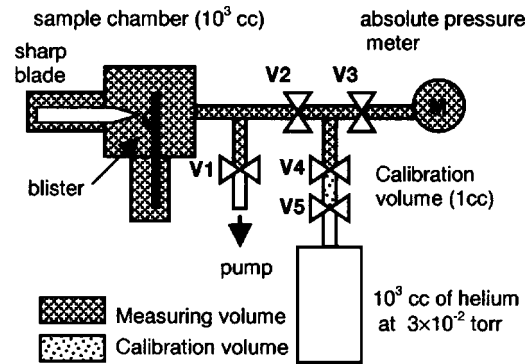


FIG. 5. Schematic presentation of the setup designed to measure the gas pressure of the blisters.

side of the laser the sample was covered with a glass plate. That prevented the blister cap from being blown away because of the shock wave.

To investigate the effect of the pulse duration a series of experiments were executed with another IR YAG laser with a pulse duration of 0.5 ms. Most of the measurements of the blister profile were performed with the stylus profiler DEKTAK 8 from Veeco. Additionally the blister shape was characterized with the help of a confocal microscope and a field-emission gun (FEG) scanning electron microscopy (SEM) Philips XL-30. The measurements performed with the stylus profiler proved to be the most practical.

In order to measure the amount of gas inside the blisters the setup schematically shown in Fig. 5 was designed. The setup consists of a sample holder, fixed on a linear motion, and a sharp blade fixed on a combination of a rotary and a linear motion. The latter enables to cut a blister located at any point on the sample without exposing the sample to air. Usually each sample contained 20 to 30 blisters. The sample chamber is connected to an absolute pressure meter. The gas from the blister is exposed to the measuring volume (in Fig. 5 valves V1 and V4 are closed, and V2 and V3 are opened). It results into a change of the absolute pressure. The volume of a typical blister with the height $H=30 \mu\text{m}$ is about $4.5 \times 10^{-6} \text{cc}$. The volume of the sample chamber together with the pressure meter and the connecting tubes is of an order of 10^3cc , measured by exposing 1 cc of helium at known pressure into the same volume and monitoring the change of the pressure. Thus, assuming that the original pressure inside the blister is 10^3torr , after exposing this amount of gas into the sample chamber the expected change in pressure is $\Delta p = 4.5 \times 10^{-6} \text{torr}$. Such changes are very close to the sensitivity limit of the pressure meter and also require that the pressure inside the sample volume is at least ten times lower.

The calibration of the pressure meter was carried out as follows: 1 cc of helium at the pressure of $3 \times 10^{-2} \text{torr}$ was sampled from the calibration vessel. The volume of the calibration vessel is 1000 cc and every sampling does not affect the pressure of gas inside the vessel. Then the gas was released into the measuring volume and the changes in the absolute pressure were recorded.

IV. EXPERIMENTAL RESULTS

A number of blister profiles measured with the stylus profiler Dektak 8 are shown in Fig. 6. The fit of the profiles

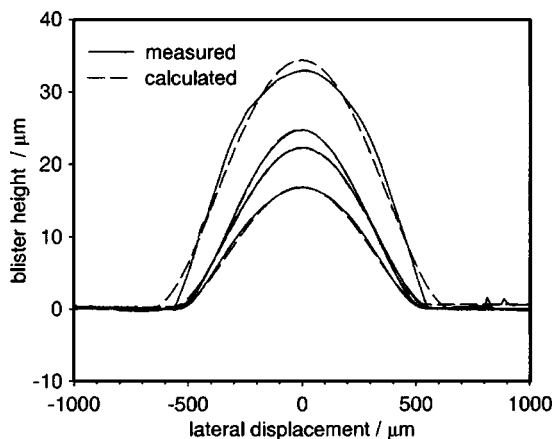


FIG. 6. The blister profilers measured with the stylus profiler Dektak 8 (solid line) and fitted with Eq. (7) (dashed line).

is performed by using Eq. (7) and is shown with the dashed line. It is not surprising that for larger blisters the fit is not perfect. The model used is valid only for stiff plates, i.e., no stretching of the plate is allowed and all the deformation energy is stored as pure bending of the plate. The condition for dropping the stiff plate model is $H \geq 0.3t$,¹⁴ and the membrane model should be applied. H is the blister height and t is the thickness of the plate. The polymer film thickness used in the experiments is 30 μm , suggesting that the stiff plate model is valid for the blisters not higher than 9 μm . Another reason for the observed discrepancy in the fit is a possible plastic deformation of the film, which is likely to take place at higher strains.

From the fit of the blister profile the following two parameters are obtained: the blister height H and the blister width b and these values are used to calculate the pressure inside the blister and the work of adhesion. As aforementioned the gas pressure inside the blister can be estimated from the blister profile measurements using Eq. (6). On the other hand, the blister pressure can be measured also independently providing a good possibility of validating the model.

A typical series of measurements of gas released from

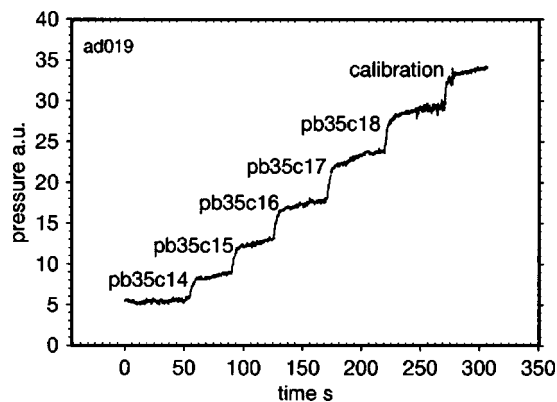


FIG. 7. The results of the measurements of gas contents in the blisters. Every opening of a blister results in a step in the output signal recorded by the pressure meter. In order to calibrate the pressure meter, a known amount of gas is allowed inside the system, and the corresponding step in the pressure signal is used for calibration.

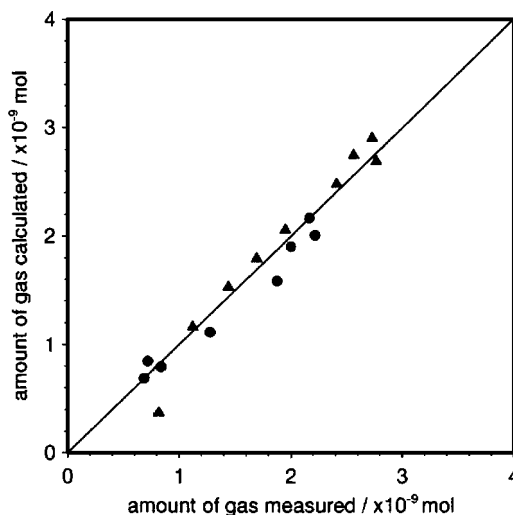


FIG. 8. Amounts of gas in the blisters are measured and calculated according to Eq. (19). Two different series of measurements are designated by different symbols.

the blisters are presented in Fig. 7. Every step in the output signal of the pressure meter corresponds to the opening of a blister. In order to calibrate the pressure meter, a known amount of gas (helium) is allowed inside the system, and the corresponding step in the pressure meter signal is recorded. Note that in these experiments, not the pressure but the amount of gas enclosed inside the blisters is measured.

The profiles of the blisters were measured with the stylus profiler before putting the sample into vacuum. The amount of gas (in mole) is estimated from the shape of the blister [Eqs. (6) and (13), for the blister pressure and volume, respectively] with

$$\frac{pV}{RT} = \left(p_{\text{atm}} + \frac{24D \cdot 16H}{b^4} \right) \frac{8}{15} \frac{abH}{RT}, \quad (21)$$

where R is the universal gas constant. The amount of gas, both measured and calculated, is shown in Fig. 8 and a fair agreement is obtained. In a number of experiments the gas released from the blister was analyzed with the help of the quadrupole mass spectrometer. The mass spectrum obtained, together with the mass spectra of the rest gas (background measurement), is presented in Fig. 9. A helium peak is present in the spectrum, because the calibration of the pressure meter was performed with helium gas. Other obvious

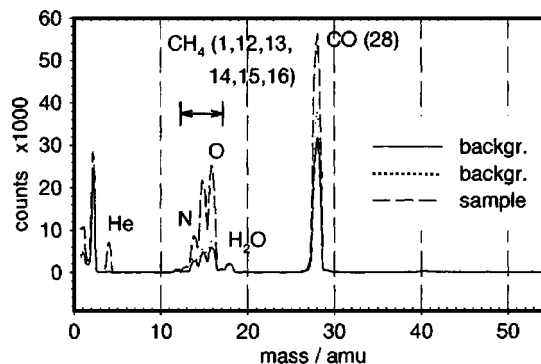


FIG. 9. Mass spectra of the rest gas and the gas released from the blisters.

contributions in the spectrum are observed at masses 1, 14, 15, and 16. Usually these contributions are ascribed to CH₄. The fact, that hydrogen contributes only to mass 1 and not to mass 2, suggests that it is formed directly in the mass-spectrometer source from the decomposition of CH₄. If hydrogen did permeate through the blister wall, it still had to recombine at the polymer surface to form H₂, and only after that could reach the quadrupole, contributing to both H₂ and H. This was not observed. After the evaporations of a PET molecule $(-O-C_2H_4-O-CO-C_6H_4-CO-)_n$, one obtains four oxygen atoms, ten carbon atoms, and eight hydrogen atoms. Thus, after forming CH₄ there are oxygen and carbon atoms left. The latter can form CO (mass 28) which is also present in the spectrum. Larger molecules, such as CH₄ and CO, are very unlikely to permeate through the blister wall. That is in line with the experiments showing a very moderate decrease in the gas content after the blisters were kept in vacuum for considerable time.

V. DISCUSSION

The objective of this experimental study is to characterize the adhesion properties of the interface. As aforementioned each laser shot produces two blisters with an unirradiated strip of a polymer between, still attached to the substrate, as shown in Fig. 4. After matching the profiles of the blisters to Eq. (7) and defining the blister pressure, the maximum tensile stress at the blister boundary has been calculated [Eq. (11)]. Every test consists of a series of shots with a stepwise increase of the pulse energy, resulting in a higher blister pressure, and thus higher stresses are exerted on the strip. Consequently, the last shot that does not result in delamination of the strip provides a lower bound estimate of the stresses necessary for delamination of the film. The experimental procedure is illustrated in Fig. 10. Figure 10(a) shows the blister profiles measured in the series. At the bottom curve the stresses applied to the bottom part of the strip are plotted as a function of the laser-pulse intensity. Before the delamination takes place two curves are present, one for each blister. After the delamination the blisters merge in one and one curve is left. The kink in the curve corresponds to the moment of delamination, providing the low bound estimate of the stresses necessary to delaminate the film: $\sigma_y^{max} = 17.0 \pm 1.0$ MPa. By using Eqs. (17) and (18), the stresses required for delamination can be converted to the practical work of adhesion or the work of fracture, $G = 2.3 \pm 0.2$ J/m².

To discuss the possible plastic deformations of the film during delamination, first consider temperature distribution in the substrate after the laser pulse,¹⁵

$$T(z,t) = \left(\frac{2I}{K}\right) \sqrt{kt} \operatorname{ierfc}\left(\frac{z}{2\sqrt{kt}}\right) - [t > t_p] \times \left(\frac{2I}{K}\right) \sqrt{k(t-t_p)} \operatorname{ierfc}\left[\frac{z}{2\sqrt{k(t-t_p)}}\right], \quad (22)$$

where $k = K/\rho C_p$ is the thermometric conductivity, K is the thermal conductivity, C_p is the specific heat at constant pressure, t_p is the pulse duration, and I is the unreflected part of incident irradiation.

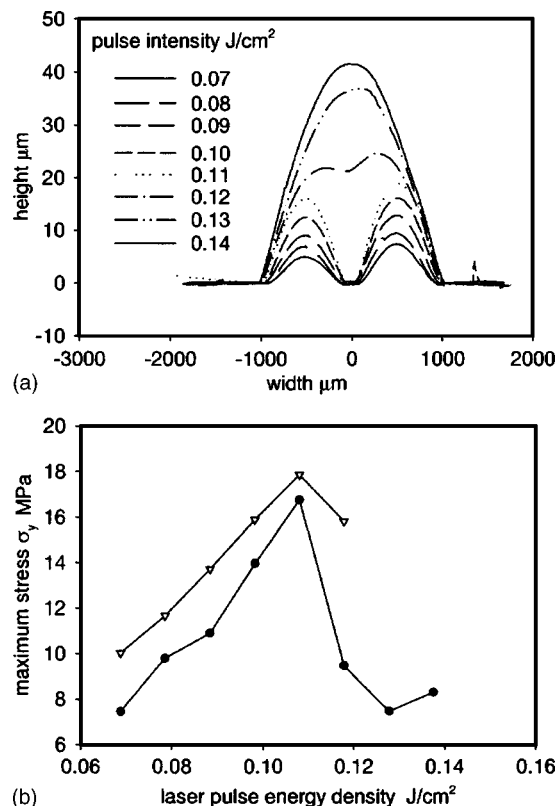


FIG. 10. (a): Blister profiles measured with the stylus profile meter. (b): tensile stress at the blister boundary (applied to the unirradiated strip) calculated for every blister. The kink in the curve corresponds to the moment of delamination.

Using Eq. (22) the temperature in the substrate (1 μm deep from the interface) was calculated for various pulse durations. The results are presented in Fig. 11.

It is quite clear that in order to create the ideal conditions for the blister formation, the time the substrate is kept above the polymer melting temperature should be as short as possible. From Fig. 11 it is seen that the removal of heat from the interface region due to thermal conduction is a very fast process and has a characteristic time less than 1 μs. That means that the laser pulses with longer duration would keep the substrate at high temperatures for an unnecessarily long time. That explains why the experiments carried out with the

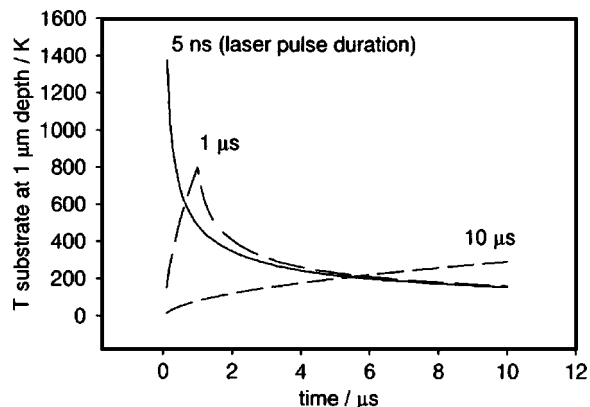


FIG. 11. The temperature of the substrate (at 1-μm depth below the interface) during and shortly after the laser pulse of various durations.

laser with pulse duration of 0.5 ms were not successful. The blisters were well created but a considerable plastic deformation was observed.

There are two other characteristic time scales that should be taken into consideration. First, the characteristic time of the blister formation can be estimated as the time necessary for a sound wave to travel a distance comparable to the typical blister height, $\tau_s = H/v_s = 50 \times 10^{-6} \text{ m} / 340 \text{ m/s} \approx 1.5 \times 10^{-7} \text{ s}$. Second, polymers are known to exhibit viscoelastic behavior as a response to a perturbation, which varies with time. It means that for relatively short perturbations elastic behavior is observed, while if the perturbation slowly changes with time, a viscous flow of the polymer is observed. The switch between the elastic and viscous responses is defined by the relaxation time τ_r . In practice viscous behavior involves different physical processes, each of which is characterized by a specific relaxation time. Regarding the time scales the processes are grouped in three major categories: α , β , and γ .¹⁶ The fastest γ -relaxations are related to fast relaxations through flipping of the sidegroups or change of conformations. Those are defined by the local stress fields on the scale of a monomer and do not depend on the size of the polymer chain. Thus, these processes cannot provide any mass transfer (mass flow), capable to change the shape of the blister. They can, however, account for a relaxation of a certain part of the elastic energy of the deformed polymer, which in turn can result in the change of the blister shape. The typical value for relaxation time of the γ processes τ_r at the room temperature is $\tau_r \geq 3 \times 10^{-6} \text{ s}$.¹⁶ The fact that the characteristic time of blister formation is less than the relaxation time $\tau_s \ll \tau_r$ provides the possibility to treat the polymer as an elastic media.

Although even γ relaxation is very unlikely to take place during the blister formation and subsequent delamination, a certain amount of relaxation can occur between the moment the blister is formed and the moment the blister profile is measured (typically about 1 or 2 hs). α and β relaxations do involve macroscopic displacements of the polymer chains but they take place on a far longer time scale. The α relaxations, which are related to glass-rubber transition, have the typical relaxation time of about 100 s at the glass transition temperature T_g .¹⁶ At the room temperature in the time window used in the presented experiments, however, α processes can be neglected. Many profile measurements repeated after 1–2 months did not show any noticeable change in the blister shape. However, a certain amount of plastic deformation of the blister wall does take place. In several experiments we broke the blisters by making a small pinhole in the blister wall releasing the gas. The blisters did decrease in size but did not disappear completely. Another source of plastic deformations not considered so far is the process of delamination described as crack propagation along the inter-

face of two media.^{10,11} The effect of the plastic deformation at the crack tip will be included in a future model description.

VI. CONCLUSIONS

The laser-induced delamination was used to study the adhesion of PET coatings on steel substrate. The main advantage of the method, as compared to the conventional blister test, is that already existing coatings can be measured, because no preparation of the substrate is necessary. Second, the formation of the blisters takes place in microseconds. On this time scale the polymer manifests pure elastic behavior. Thus the contribution of the plastic deformation to the measured practical work of adhesion is limited.

The experimentally obtained blister profiles and the blister pressures were compared to those predicted by the proposed elastic model. The predicted results are in good agreement with the experiments.

The adhesion of the PET film is characterized in terms of the stress required to delaminate the film and the practical work of adhesion or fracture energy. The tensile stress obtained from the measurements of $\sigma_y^{\text{max}} = 17.0 \pm 1.0 \text{ MPa}$ corresponds to the practical work of adhesion of $G = 2.3 \pm 0.2 \text{ J/m}^2$.

ACKNOWLEDGMENTS

The authors owe a special debt of gratitude to Professor A. van Veen, whose contribution at the early stage of this project is invaluable. Professor A. van Veen suddenly passed away in the beginning of this year. The authors would like also to thank Professor L. Siebbeles who kindly permitted them to use the Dektak stylus profiler and offered necessary technical support. This work was supported by the Netherlands Technology Foundation (STW), Project No. GTF.4901.

¹M. L. Williams, *J. Appl. Polym. Sci.* **13**, 29 (1969).

²B. Cotterell and Z. Chen, *Int. J. Fract.* **86**, 191 (1997).

³B. J. Briscoe and S. S. Panesar, *Proc. R. Soc. London, Ser. A* **443**, 23 (1991).

⁴J. G. Williams, *Int. J. Fract.* **87**, 265 (1997).

⁵H. M. Jensen, *Int. J. Fract.* **94**, 79 (1998).

⁶J. S. Meth, D. Sanderson, C. Mutchler, and S. J. Bennison, *J. Adhes.* **68**, 117 (1998).

⁷A. Fedorov, A. van Veen, R. van Tijum, and J. Th. M. De Hosson, *Mater. Res. Soc. Symp. Proc.* **795**, (2004).

⁸L. S. Pen and E. Defex, *J. Mater. Sci.* **37**, 505 (2002).

⁹D. E. Packman, *Int. J. Adhes. Adhes.* **23**, 437 (2003).

¹⁰Y. Wei and J. W. Hutchinson, *Int. J. Fract.* **93**, 315 (1998).

¹¹I. Georgiou, H. Hadavinia, A. Ivankovic, A. J. Kinloch, V. Tropsa, and J. G. Williams, *J. Adhes.* **79**, 239 (2003).

¹²A. A. Volinsky, N. R. Moody, and W. W. Gerberich, *Acta Mater.* **50**, 441 (2002).

¹³D. D. Eley, *Adhesion* (Oxford University Press, New York, 1961).

¹⁴E. Fentsel and Th. Krauthammer, *Thin Plates and Shells* (Marcel Dekker, New York, 2001).

¹⁵M. von Allmen, *Laser-Beam Interactions with Materials* (Springer, New York, 1995).

¹⁶G. Strobl, *The Physics of Polymers* (Springer, New York, 1997).